Geo-Mechanical Modelling for Optimization of Rock Slope in an Opencast Coal Mine

Masoud Monjezi
Organization, Tehran, Iran

T. N. Singh
IT-BHU, Varanasi, U.P., India

Amit Pandey
IT-BHU, Varanasi, U.P., India

Saurabh Puri
IT-BHU, Varanasi, U.P., India

Follow this and additional works at: https://scholarsmine.mst.edu/icchge

Part of the Geotechnical Engineering Commons

Recommended Citation

GEO-MECHANICAL MODELLING FOR OPTIMIZATION OF ROCK SLOPE IN AN OPENCAST COAL MINE

Dr. Masoud Monjezi
Organization
Tehran, Iran

Dr T. N. Singh   Mr. Amit Pandey   Mr. Saurabh Puri
IT-BHU
Varanasi, U.P.(India)

ABSTRACT

Jharia Coalfield, in India, is a prime storehouse of the coking coal. It contains as many as thirty contiguous seams. Multiplicity of seams has contributed to a number of problems, fire, inundated workings, goaf out area and disturbed strata condition. However, due to various geotechnical problems, it was not possible to fully extract coal by underground mining method. Opencast mining is now planned for extraction of virgin coal seams upto an ultimate depth of 500 m for ensuring maximum resources recovery. There are various modeling methods to analyze the behaviour of slopes. To achieve the objective for ensuring the safe slopes with steepest possible angle, the prototype of one of the mine was simulated in physical model i.e. Equivalent material model (EM) incorporating all the pertinent characteristics of rock mass, mining method and geological discontinuities properties. The results of EM are corroborated by Numerical method using Computer code FLAC- 2D. It was observed that when slope reached near the bottom seam the resultant vector of various monitoring points showed toppling tendency of slopes whereas high stress concentration was observed in the toe region and decreases towards the surface.

INTRODUCTION

In India, coal is a prime source of energy and continued to be the main source of energy in near future also. To bridge the gap between demand and supply of minerals, fossil fuels and metals because of continuous depletion of high grade mineral deposits in recent years and the massive increase in the raw material consumption has boosted up the open cast mining of even minor profitable thin deposits upto a greater depth.

The large and deep open pits mines have been planned and its design is always crucial with particular reference to selection of slope angle, bench width and overall pit slope. The economics of such deep and extensive mines is always dependent on the overall slope angle of pit, because the slope pre determines the quantity and cost of waste material removal necessary to recover the coal seam. (Goodman, 1980; Hoek and Bray, 1977).

These problems are more stimulated in the Jharia coalfield, Jharkhand, India. These coal seams were exploited earlier in haphazard manner by underground and surface mining methods. Due to its good quality and demand, opencast mining is being urged for extraction of locked coal as well as virgin seam upto 480-m depth. The major problem conceived will be the repercussion of old voids on stability of pits so that maximum resource recovery can be consummated. Too flat slope means extra excavation of extra waste rock, on the other hand, steepening of slope may save a huge sum of money, but excessive steepening may result in slope failure causing loss of life, detrimental to equipment and properties. Too much steepening of a slope will escalate the number of lost time hours, haulage road congestion and accidents (Singh, 1990).

The economic relationship between steepening of the slope and decreasing waste removal requirements is one of the most important factors in the design of open pit slope, the ultimate objective being to make the steepest possible safe slope. In order to effectuate the objective of making safe slopes with steepest possible angle, the analysis of existing slopes about their stability or for evolving proper design is expedient.

EQUIVALENT MATERIAL MODELLING (EMM)

Equivalent material modeling (EM) is one of the most effective tools of modeling of rock mass and solving problems related to surface and underground mines. In mines, strata movements and stress variations around mine openings can be investigated using equivalent material models. They are constructed by adequately

scaling down the inherent properties of rock mass and give valuable information regarding pit slope (Singh, 1986 and Singh & Singh, 1991a&b).

Mechanism of Equivalent Material Modeling

In EMM the fundamentals of dimensional analysis is employed. The power of dimensional analysis lies in the fact that certain quantities can be evaluated even when the complete equation including the contents is not known. If a problem can be specified by number of independent variables, a dimensionless matrix can be formed, the rank of which subtracted from the number of variables give the number of dimensional products on π form in complete set. The first step towards model design is to consider the equations, which describe physical phenomenon. Consider a variable y_1 which is dependent on the number of other variables y_2, y_3,...,y_n. Their general characterizing equation may be written as,

$$y_1 = f(y_2, y_3, y_4, ..., y_n) \quad ....1$$

The above equation is dependent on measurement of various parameters. If these parameters can be converted into dimensionless parameters, then it can define other systems also. It can be converted on the basis of Buckingham Pie Theorem (Murphy, 1950; Bridgman, 1963). The theorem states that if there are 'n' variables with 'a' number of dimensions, the number of dimensionless terms 'k' will be as follow,

$$k = n-a \quad ....2$$

The general equation for the system can be expressed as,

$$\pi_{1p} = f(\pi_{2p}, \pi_{3p}, \pi_{4p}, ..., \pi_{kp}) \quad ....3$$

Same equation can be written for a model, which is defined by above parameters as,

$$\pi_{1m} = f(\pi_{2m}, \pi_{3m}, \pi_{4m}, ..., \pi_{km}) \quad ....4$$

Dividing equations 2.3 and 2.4, dimensionless equation can be derived as,

$$\pi_{1p}/\pi_{1m} = f(\pi_{2p}, \pi_{3p}, \pi_{4p}, ..., \pi_{kp}) / f(\pi_{2m}, \pi_{3m}, \pi_{4m}, ..., \pi_{km}) \quad ....5$$

according the law of similitude, if the model is designed and operated such that

$$\pi_{2p} = \pi_{2m}, \pi_{3p} = \pi_{3m}, \pi_{4p} = \pi_{4m}, ..., \pi_{kp} = \pi_{km} \quad ....6$$

Then the two functions will be equal,

$$f(\pi_{2p}, \pi_{3p}, \pi_{4p}, ..., \pi_{kp}) = f(\pi_{2m}, \pi_{3m}, \pi_{4m}, ..., \pi_{km}) \quad ....7$$

and thus,

$$\pi_{1p} = \pi_{1m} \quad ....8$$

The equation 7 gives the boundary condition for the designing equations. If this equation is satisfied, equation 8 will be the predicting equation. With the help of this equation the behaviour of proto-system can be predicted from the derived results of the models. The factors, which affect deformations in a mining system, are written in the form of equation as,

$$\delta = f(l, w, h, d, E, \sigma, \lambda, T) \quad ....9$$

Using the fundamentals of dimensional analysis, above equation can be written as,

$$k \, \delta^{k}{}_1 l^{k}{}_2 w^{k}{}_3 h^{k}{}_4 d^{k}{}_5 E^{k}{}_6 \sigma^{k}{}_7 \lambda^{k}{}_8 T^{k}{}_9 = 1 \quad ....10$$

where, $k_1, k_2, ... , k_9$ are constants.

By substituting the dimensions, the general equation may be written as:

$$\delta / l = f(b / l, l / h, h / d, \rho l / E, \sigma / E) \quad ....11$$

This formula can be applied for both the model and prototype and it can be written as,

$$\delta_m / l_m = f(b_m / l_m, l_m / h_m, h_m / d_m, \rho_m l_m / E_m, \sigma_m / E_m)$$
$$\delta_p / l_p = f(b_p / l_p, l_p / h_p, h_p / d_p, \rho_p l_p / E_p, \sigma_p / E_p)$$

To satisfy similarity, following conditions should be available,
$b_m / l_m = b_p / l_p$

$$.......................................12$$

$l_m / h_m = l_p / h_p$

$$.......................................13$$

$h_m / d_m = h_p / d_p$

$$.......................................14$$

$\rho_m l_m / E_m = \rho_p l_p / E_p$

$$.......................................15$$

$\sigma_m / E_m =, \sigma_p / E_p$

$$.......................................16$$

$\nu_m = \nu_p$

$$.......................................17$$

$\phi_m = \phi_p$

$$.......................................18$$

Equations 12-14 are geometrical parameters, whereas equations 15-16 are related to Physico-mechanical properties. Equations 15 & 16 can be written as,
$E_p / E_m = \rho_p l_p / \rho_m l_m$

$$............19$$

as $b_m / b_p = l_m / l_p = h_m / h_p = d_m / d_p = \alpha$

$$.......................................20$$

Equation 20 will become,
$$E_p/E_m = \rho_p/\rho_m \cdot 1/\alpha = \sigma_p/\sigma_m \quad ....21$$
$$\sigma_m = \alpha \cdot \rho_m/\rho_p \cdot \sigma_p \quad ....22$$
For kinetic similarity,
$$l_p \, T^{-2}{}_p = l_m \, T^{-2}{}_m \quad ....23$$
$$or,$$
$$T_m/T_p = \sqrt{l_m/l_p} = \sqrt{\alpha} \quad ....24$$
The other dimensionless parameters like poisons ratio (ν) and angle of friction (φ) should be same for both model and prototype.

The prediction equation will then yield,

$$\delta_p = l_p/l_m \cdot \delta_m \quad \ldots\ldots\ldots\ldots\ldots 25$$

Design of Equivalent Material Model

The design of EM model is based on Physico-mechanical properties of various rocks constituting the rock mass, orientation of major joint sets determined in the field. Joint parameter i.e. joint spacing (K_1), nature of joint surface (K_2), nature of filling (K_3) and joint aperture (K_4) was recorded from the exposed phase of the mine "A". The jointing parameters were quantified as suggested by Singh & Singh (1992). The observed jointing parameters are given in Table 1 & 2.

Rock Quality Index R was determined and Rock Weakening Coefficient (i) was calculated for each layers. The Rock Mass Strength (σ_P) was calculated from the sample strength (σ_S), geometrical scale of modeling (α) and dynamic scale of modeling (α_d).

$$K = k_1 \times k_2 \times k_3 \times k4 \quad \ldots\ldots\ldots\ldots\ldots\ldots 26$$
$$= 0.7 \times 0.9 \times 0.7 \times 0.9$$
$$= 0.40$$

The Rock mass Strength (σ_P) was calculated as follows:
$$i = R \times K \quad \ldots\ldots\ldots\ldots\ldots\ldots 27$$
$$\sigma_P = \sigma_S \times i \ldots\ldots\ldots\ldots\ldots\ldots 28$$

The required equivalent material properties (σ_m) were computed for various litho units of the rock mass.

$$\sigma_{m=} \sigma_P \times \alpha \times \alpha_d \quad \ldots\ldots\ldots\ldots\ldots\ldots 29$$

Table 1. Weakening coefficient of coal measures formations.

Parameter	Rock mass Classification			
	Poor	Moderate	Good	Strong
Rock Quality Designation (RQD)	40%	40-60%	60-80%	80%
Index R	0.4	0.4-0.6	0.6-0.8	0.8
Joint spacing	Close Upto 0.3m	Moderate 0.3-1.0m	Wide 1.0-2.0m	Remote 2.0m
Index K1	0.7	0.8	0.9	1.0
Joint surface	Polished	Smooth	Rough	Dormant
Index K2	0.7	0.8	0.9	1.0
Joint Filling	Open Asperity	Soft filling	Tight filling	
Index K3	0.7	0.8	0.9	1.0
Joint aperture(mm)	5.00	1-5	0.1-1.0	Upto0.1
Index K4	0.6	0.7	0.8	0.9
Weakening coefficient	0.1	0.1-0.2	0.2-0.5	0.5-0.7

Table 2. Quantification of joint parameters (after Singh, 1986)

Parameter	Index	Field observation	Index value
Joint spacing	k_1	Less than 0.3m	0.7
Joint surface	k_2	Rough	0.9
Joint filling	k_3	Open	0.7
Joint aperture	k_4	Less than 0.1 mm	0.9

The required material strength was computed for various section of the rock mass. The model was constructed in a 2.0 x 2.0 x 0.20 m steel frame pivoted at one end. The frame was provided with tilting arrangement. The EM was developed by mixing Silica sand, Mica power, Plaster of Paris and Borax powder with water with varying proportion. The frame was tilted at 8^0 for simulating bedding plane inclination. The major joint sets were simulated in the model with the help of joint simulator. The layer thickness was kept 1.0 cm when RQD of the rock unit is 40% and if it is more than 40% then 2.0 cm layer thickness simulated in the model.

This equivalent material (EM) model was constructed to study the behaviour of pit slope in normal conditions, where stresses within the model are induced by gravitational forces only. Excavation was done as per the plan shown in Fig 1. Location of various monitoring points is also shown in this Figure. Bench width to height ratio of each individual bench was kept 1:3 in various stages of excavation.
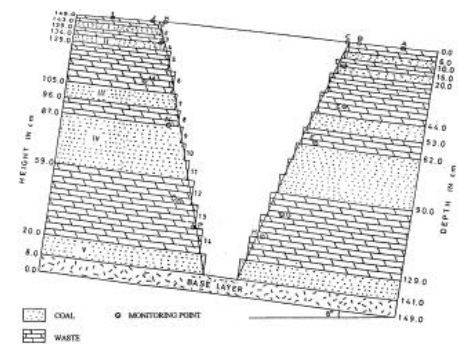

Fig 1. Excavation plan with location of various monitoring points

Results and Discussion

For each monitoring point, displacements in the X-Y direction were recorded on the top and in the plane of the model. Table 3 & 4 shows the records of displacement recorded on the rise side and the dip side, respectively. Slope process of rise and dip side slope is discussed.

Rise Side Slope

Excavation was done upto 90.0 cm depth (10th bench) without any sign of instability. The displacement vectors were in the range of 0.02 mm to 0.17 mm, at various monitoring points upto this stage of excavation. At each successive stages of excavation, direction of displacement vectors increased. Maximum displacement vectors at monitoring points L and N changed from 0.10 mm/16.70° and 0.17 mm/30.96° to 0.12 mm/19.98° and 0.25 mm/31.76°, respectively, after excavation of the 11th bench. The higher magnitude of displacement in the coal seam was probably due to the strata conditions. Coal seam was situated in between the two competent beds of shale and sandstone. Coal seam shows higher deformation as compared to shale and sandstone due to varying deformation moduli. However, no visible failure was observed in the model.

Further deepening of the pit indicates appreciable change in displacement vectors particularly at points, which were near to the slope face. Fig 2 shows excavation upto 12th bench (116.0 cm depth) and 14th bench (141.0 cm depth). From the Table.3 it is evident that for each monitoring point, displacements in X and Y direction increases as depth increases. It was probably due to the fact that by increasing depth stress concentrations were higher and can accelerate the deformation in the model. Similar observations were reported by Singh & Singh (1991 a).

Fig 2. Excavation down to 14th bench (141.0 cm depth).

Table 3. Records of displacements in X-Y direction in the EM model I having bench width to height ratio 1:3 (rise side)

Events		Displacements at observation points (mm)							
		I	J	K	L	M	N	O	P
3rd bench	x	-	-	0.00	0.00	0.00	0.00	0.00	0.00
	y	0.0	0.01	-	0.01	0.00	0.00	0.00	0.00
5th bench	x	-	-	0.00	0.00	0.00	0.00	0.00	0.00
	y	0.01	0.01	-	0.02	0.01	0.01	0.00	0.00
7th bench	x	-	-	0.01	0.00	0.01	0.00	0.00	0.00
	y	0.03	0.05	-	0.06	0.07	0.03	0.01	0.01
10th bench	x	-	-	0.02	0.03	0.07	0.09	0.00	0.00
	y	0.06	0.09	-	0.10	0.12	0.15	0.05	0.04
11th bench	x	-	-	0.02	0.04	0.09	0.13	0.03	0.00
	y	0.10	0.13	-	0.11	0.18	0.21	0.12	0.07
12th bench	x	-	-	0.03	0.06	0.10	0.14	0.11	0.03
	y	0.13	0.16	-	0.19	0.25	0.27	0.30	0.14
13th bench	x	-	-	0.04	0.09	0.14	0.22	0.27	0.33
	y	0.17	0.19	-	0.23	0.27	0.39	0.42	0.46
14th bench	x	-	-	Out	0.12	0.18	0.30	0.40	0.57
	y	0.21	0.33	Out	0.29	0.34	0.43	0.48	0.62
Lateral widening	x	-	Out	Out	Out	0.30	0.52	0.61	0.73
	y	0.23	Out	Out	Out	0.52	0.68	0.72	0.81

Lateral widening of the pit by 12.0 cm did not pose any physical instability problem in the rise side slope (Fig 3.). However, various monitoring points show increasing trend of displacement vectors. Displacement vectors at monitoring points O and P in the lower portion of the slope varied from 0.63 mm/ 39.81° to 0.94 mm/ 40.27° and 0.84 mm/42.59° to 1.09 mm/42.03°, respectively. By increasing the depth of excavation, the direction of these displacement vectors indicated initiation of toppling movement.

Dip Side Slope

Deepening of the pit upto last stage of the excavation including lateral widening of the pit was carried out without any observable failure in the model. Like rise slope, dip side slope also did not show any physical failure upto the depth 141.0 cm (14th bench). After each successive stages of excavation,
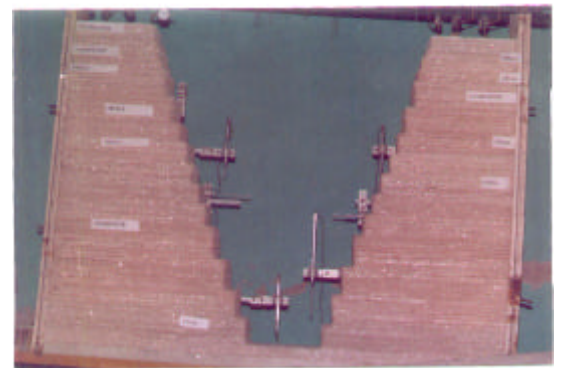

Fig 3. Strata conditions after lateral widening.

displacements in X and Y direction, for different monitoring points were recorded (Table 4). Displacement vectors at various monitoring points increased with increasing depth in this side of the slope. Upto the stage of excavation of 10th bench, the maximum displacement vector was at monitoring point F with a magnitude of 0.13 mm and direction of 12.99° from the Y-axis, which is perpendicular to the bedding planes. After lateral widening of the pit, the monitoring point H showed the maximum displacement of 0.64 mm and 0.74 mm in X and Y directions, respectively (Table 4). It is evident that

the displacements are smaller as compared to the rise side slope, because bedding planes are dipping against the slope face. No perceptible difference in displacement vectors of rise and dip slopes was observed. It may be attributed to gentle angle of bedding planes.

Table 4.Records of displacements in X-Y direction in the EM model I having bench width to height ratio 1:3 (dip side)

Events		Displacements at observation points (mm)							
		A	B	C	D	E	F	G	H
3rd bench	x	-	-	0.00	0.00	0.00	0.00	0.00	0.00
	y	0.00	0.0	-	0.00	0.00	0.00	0.00	0.00
5th bench	x	-	-	0.00	0.00	0.00	0.00	0.00	0.00
	y	0.00	0.01	-	0.00	0.00	0.00	0.00	0.00
7th bench	x	-	-	0.00	0.00	0.00	0.00	0.00	0.00
	y	0.01	0.02	-	0.01	0.03	0.01	0.00	0.00
10th bench	x	-	-	0.01	0.01	0.01	0.03	0.00	0.00
	y	0.03	0.07	-	0.03	0.06	0.13	0.02	0.02
11th bench	x	-	-	0.01	0.02	0.06	0.09	0.01	0.00
	y	0.07	0.09	-	0.06	0.15	0.18	0.07	0.05
12th bench	x	-	-	0.02	0.04	0.07	0.09	0.08	0.01
	y	0.11	0.12	-	0.16	0.23	0.23	0.27	0.08
13th bench	x	-	-	0.02	0.05	0.10	0.16	0.19	0.22
	y	0.13	0.14	-	0.18	0.24	0.34	0.37	0.40
14th bench	x	-	-	Out	0.09	0.15	0.28	0.32	0.49
	y	0.16	0.19	Out	0.22	0.27	0.39	0.41	0.58
Lateral widening	x	-	Out	Out	Out	0.22	0.47	0.55	0.64
	y	0.18	Out	Out	Out	0.46	0.61	0.68	0.74

NUMERICAL MODELLING

The advantage of numerical modeling is that in this case we do not presuppose a failure surface, but rather the failure surface corresponding to the minimum factor of safety develops naturally as a function of the combination of material properties and geometry. To understand the slope stability problems, numerical methods are beneficial as compared to the limit equilibrium methods as both displacements and stresses can be obtained from these methods and different constitutive models can be employed for a specific problem. In the present paper the finite difference programme FAST LAGRANGIAN ANALYSIS OF CONTINUA (FLAC) is used (Itasca, 1990).

Theory of Numerical Modeling

In this paper, the rock mass is considered as jointed due to which a ubiquitous model is assigned to all the zones. This model assumes a series of weak planes embedded in a Mohr-Coulomb solid. Yield may occur in either the solid or along the slip plane, or both, depending on the material properties of the solid and planes, the stress state, and the angle of the slip planes. The ubiquitous model applies for a Mohr Coulomb material that exhibits a well-defined strength anisotropy. This

is actually a variation of the Mohr Coulomb model used for the excavations in the closely bedded strata. Along with the properties of intact rock, ubiquitous model also requires strength properties for the plane of weakness (derived from laboratory testing-triaxial and direct shear test.). The material properties used in the model should correspond as closely as possible to the values of the physical problem. The laboratory-measured properties generally should not be used directly in the model. These properties should be scaled to account for the presence of discontinuities and heterogeneities present in the rock. Deformability of a rock mass is generally defined by a modulus of deformation (E_m). For the jointed rock mass the value of E_m can be estimated by treating the rock mass as an equivalent isotropic continuum. The following relation can be used to estimate E_m in the direction normal to the joint set:

$$1/ E_m = 1/ E_r + 1/ k_n^s \quad ....30$$

where,

E_m= rock mass Young's Modulus,

E_r= intact rock Young's Modulus,

k_n= joint normal stiffness, and

s = joint spacing.

A similar expression can be derived for shear modulus:

$$1/ G_m = 1/ G_r + 1/ k_s^s \quad ....31$$

where,

G_m= rock mass shear modulus,

G_r= intact rock shear modulus, and

k_s= joint shear stiffness.

Failure Criteria:

The Mohr Coulomb strength criterion is one of the most widely used strength criteria in geotechnical engineering applications (Zhao, 2000). The basic concepts of the Mohr Coulomb strength criterion suggest that the shear strength (τ) of a rock material is made up of two parts: a constant cohesion (c) and a friction varying with normal stress (σ_n).

$$\tau = c + \sigma_n .\tan f \quad ....32$$

where f is the angle of internal friction. Applying the stress transformation equations we get

$$\sigma_n = (\sigma_1 + \sigma_3)/2 + (\sigma_1 - \sigma_3)/2 .\cos 2b \quad ....33$$
$$\tau = (\sigma_1 - \sigma_3)/2 .\sin 2b \quad ....34$$

From the Mohr circle plot, the orientation of the critical plane of failure is given by

$$b = \pi / 4 + f / 2 \quad ....35$$

The critical approach for evaluating the stability of slopes is to evaluate the factor of safety. For slopes, factor of safety is often defined as the ratio of the available shear strength along the most critical failure surface to shear stress along the surface.

Result and Discussion

In the present model, a pit with an overall angle equivalent to bench width to height ratio 1:3 and ultimate depth of 141.0 m was simulated. An attempt was made to understand the behaviour of slope without application of thrust.

Rise side slope

Points along the excavation boundary were selected as monitoring points. The location of monitoring points is fixed as in the Equivalent Material Model. Major (σ_1) and minor (σ_2) principal stresses, angle of minor principal stress counter-clockwise with respect to x- direction (θ^0), maximum shear stress (τ) and displacement for different monitoring points are presented in Table 5.

Maximum displacement 0.11(56.46^0) was at monitoring point N. Angle of displacement vectors decreased with increasing depth. Displacement at monitoring points L and P was 0.08 (86.55^0) and 0.08 (43.09^0), respectively

Table 5. Stress and displacement at various monitoring points.

Points	σ_1 (MPa)	σ_2 (MPa)	θ^* (^{0})	Maximum Shear stress (MPa)	Magnitude (m)	Direction** (^{0})
L	-	-	-	-	0.08	86.55
M	0.79	0.03	0.10	0.38	0.07	66.47
N	1.11	0.03	0.27	0.54	0.11	56.46
O	1.65	0.04	0.39	0.81	0.08	45.51
P	1.80	0.20	0.61	0.80	0.08	43.09

* Angle of minor principal stress counter-clockwise from the x-direction
** Angle is measured counter clockwise in x- direction

Major principal stress contour are given in Fig. 4. Maximum and minimum stress concentration at monitoring points P on the toe region and M in the crest area are 1.80 MPa (compression) and 0.79 MPa (compression), respectively, indicating decrease in stress concentration while approaching the crest region.
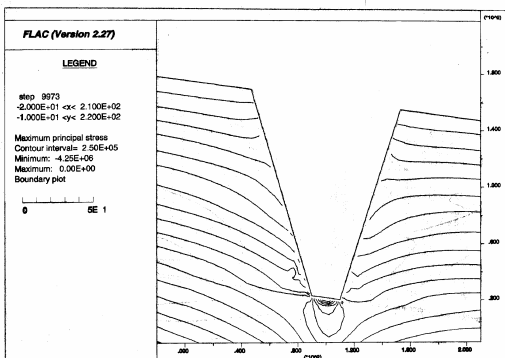

Fig. 4 Major Principal Stress Contours.

Plot of minor principal stress is given in Fig.5.The tensile stress zones are developed mostly in upper portion of the slope face. However, in the middle and lower parts, small tensile stress zones appeared all along the slope line. Numerical values of tensile stress are not significant as far as failure is concerned. Stress concentration at point P was 0.20 MPa (Tension).

Maximum shear stress (0.80 MPa) was observed at monitoring point O. The shear stress concentration decreases towards the crest of slope. It reaches 0.38 MPa at monitoring point M.

Plot of principal stresses is given in Fig 6. Confined state of stresses was changed to unconfined state due to excavation of the pit. The numerical values of minor principal stress are almost zero near to the slope face. The direction of the major principal stresses in zone of influence was towards the excavation all along slope face.
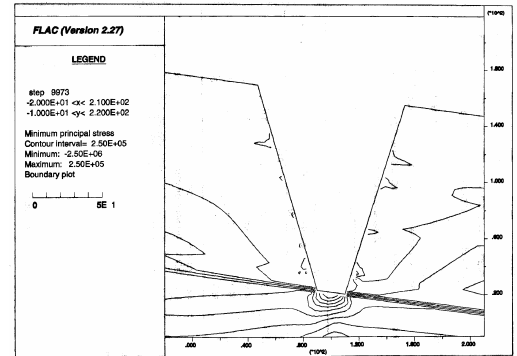

Fig. 6 Minor Principal Stress Contours.

Figure 7 shows plot of plasticity, an indicator of slope stability. It is evident that with present rock properties and pit geometry, the slope is stable. In the lower portion, at toe region, few joint elements yielded in the past. This zone has experienced plastic deformation, but restored its elastic state may be due to stress redistribution.
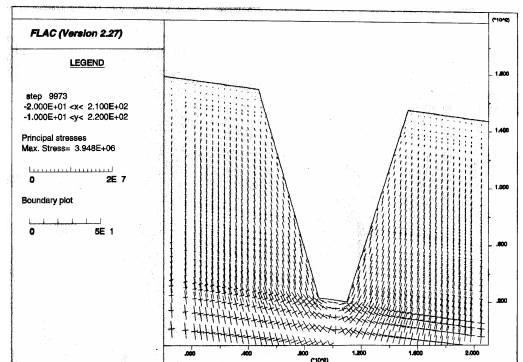

Fig. 6 Plot of Principal Stresses.

Dip side slope

The trend of decreasing angle of displacement vectors was also noticed in this side. The angle was 81.69^0 and 43.24^0 at points D and H, respectively. Maximum displacement, 0.12 m (52.08^0) was at monitoring point F in the Coal seam No. IV. (Table 6). It is evident from Figs 4 to 7 that stress distribution patterns are almost similar to the rise side. It implies that gentle angle of bedding planes does not influence stability considerably. Due to orientation of bedding planes and joints (i.e. dipping against the slope face), pit slope was more stable in this side as compared to the rise side.
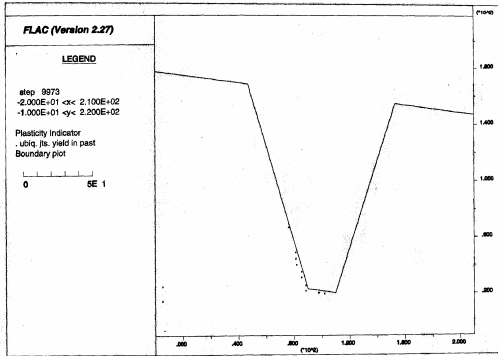

Fig. 7 Plot of Plasticity

Table 6. Stress and displacement at various monitoring points.

Points	σ_1 (MPa)	σ_2 (MPa)	θ^* (^{0})	Maximum Shear stress (MPa)	Magnitude (m)	Direction** (^{0})
D	0.30	0.01	-19.17	0.15	0.09	81.69
E	0.78	0.04	-19.36	0.37	0.08	55.53
F	1.11	0.02	-12.77	0.55	0.12	52.08
G	1.69	0.08	-15.43	0.81	0.09	44.10
H	2.06	0.02	-16.73	1.02	0.09	43.24

* Angle of minor principal stress counter-clockwise from the x-direction

** Angle is measured counter clockwise in x- direction

The factor of safety at various vulnerable monitoring points was calculated. The factor of safety at the point 'M' was just below unity and this point shows instability whereas point 'N' gives unit Factor of safety. Overall factor of safety in this stage indicates instability, which required further precautions to prevent initiation of failure.

CONCLUSIONS

- The present study provides some of the important information regarding failure mechanism of pit slope. Favorable orientation of joints towards the excavation in the rise side slope abetted the slope failure. The dip side slope was stable as compared to rise side slope due to orientation of joint and bedding planes. The excavation carried out up to last stage indicates no physical instability however resultant vectors of various monitoring points shows toppling tendency of slope. Unconfined state of stress was observed all along the slope face.

- Results obtained from EM model were good agreement with the numerical models.

- The Factor of Safety at different points on the indicates slope is just unstable. It needs precaution remedial measures for further extraction.

REFERENCES

1. Bridgman P.W.(1963) *Dimensional Analysis*, New Haven Yale University Press.
2. Goodman, R.E. (1980). *Application of rock mechanics to rock slope engineering. Introduction to rock mechanics*: 254-260. New York: J. Wiley & Sons.
3. Hoek, E. and Bray, J.W. (1977). *Rock slope engineering (3rd ed.)*: 29, 90, 93, 232-238. London Inst. of Mining and Metallurgy.
4. Itasca (1990), *FLAC Version 2.27*, Manual Minneapolis ICG.
5. Murphy G, (1950), *Similitude in Engineering*: 3-93, Renold Press, New York , Part – I.
6. Singh, T.N. (1986) *Application of equivalent material models in mines and tunnels*. Workshop on rock mechanics, problems of tunnels and mine roadways, Shrinagar, India: 4.2.1-4.3.11
7. Singh, T.N. (1990). *A study of opencast slope stability in the ground disturbed by earlier workings by equivalent material Modelling technique,* Ph.D. thesis (unpublished): BHU, Varanasi.
8. Singh, T.N. and Singh, D.P. (1991a). *Slope behaviour in an opencast mine over old underground voids*. Int. J. of Surface Mining and Reclamation, 5(4): 195-201.
9. Singh, T.N. and Singh, D.P. (1991b). *Application of scale model of equivalent material for the solution of problem related to slope stability in opencast mine*. Indian J. of Engineers, 24(4): 49-55.
10. Singh, T.N. and Singh, D.P. (1992). *Assessing stability of voids in multiseam opencast mining*. Colliery Guardian, 240 (4): 159-164.
11. Zhao J., (2000), "Applicability of Mohr- Coulomb and Hoek Brown strength Criteria to the dynamic strength of brittle rock", International Journal of Rock Mechanics and Mining Sciences, 1115-1121.